The dynamics of the reaction of $^{16}O(^1D)+D_2\ ^{18}O \rightarrow {}^{16}OD+{}^{18}OD$

William A. Guillory[a)]

Department of Chemistry, University of Utah, Salt Lake City, Utah 84112

K. H. Gericke and F. J. Comes

Institut für Physikalische and Theoretische Chemie, Universität Frankfurt a.M., D 6000 Frankfurt a.M., West Germany

(Received 9 September 1982; accepted 4 February 1983)

The detailed energy partitioning in the reaction of a metastable oxygen atom $O(^1D)$ with D_2O proceeding to two OD molecules has been studied. In order to distinguish the product state distribution between the two chemically identical product molecules OD, the oxygen atom in the heavy water molecule was labeled isotopically. The use of spectroscopic methods allows a complete analysis of the products' state distribution including such fine details as the distribution of the different Λ components and of the electron spin. The vibrational energy is almost exclusively channeled into the new (^{16}OD) bond, whereas the original (^{18}OD) bond is produced ($> 90\%$) in the ground vibrational state. Both OD radicals show a broad rotational excitation and the rotational energy is equally partitioned among the two bonds. The energy distribution over the rovibrational levels strongly reflects the influence of coincident product molecules emerging from this chemical reaction. The reaction is very direct and must proceed on a time scale which does not allow for efficient energy transfer into all the available phase space.

INTRODUCTION

The ideal of the chemical dynamicist is to characterize the elementary bimolecular process

$$A(\mathbf{P}_A, {}^Af)+B(\mathbf{P}_B, {}^Bf)\rightarrow C(\mathbf{P}_C, {}^Cf)+D(\mathbf{P}_D, {}^Df)\ , \qquad (1.1)$$

where P represents the momentum and f stands for all internal quantum states of the molecule. If we obtain the probability function which characterizes process (1.1), then all less resolved kinematic data, like the reaction rate or its dependence on temperature, can be calculated by proper statistical methods.

So far, this ideal experiment has not been performed, but present technology does allow a reasonable approximation to the characterization of such a process.

Previous examples of the atom exchange reactions

$$A+BC(\mathbf{P}_{BC}, {}^{BC}f)\rightarrow AB(\mathbf{P}_{AB}, {}^{AB}f)+C \qquad (1.2)$$

have been studied in detail.[1] The energy partitioning in the internal quantum states ${}^{AB}f$ were investigated mainly by the infrared chemiluminescence method,[2–4] while velocity and angular distributions have been performed by the use of molecular beam techniques. For process (1.2), it suffices in principle, to measure the molecular distributions, since the coincident atomic product is determined by conservation of energy and momentum (for given initial conditions).

It has been recently demonstrated that photon dissociation of selected polyatomic molecules provides a convenient source of atomic, diatomic, and triatomic radicals for the study of elementary bimolecular reactions. Reactants can be produced in a collisionless manner within a single laser pulse (IR, VIS, UV). The rate of removal of a given rovibronic state of these reactant species is most conveniently probed using tunable dye lasers. For carefully chosen reactants, both products [C and D in process (1.1)] can be probed with spectroscopic methods. One of the most detailed studied reactions is the reactive collision of metastable oxygen atoms with water molecules[5–10]

$$O(^1D)+H_2O\rightarrow OH+OH\ . \qquad (1.3)$$

This reaction offers an opportunity for a detailed study of the more challenging case of four-body dynamics

$$A+BCD\rightarrow AB({}^{AB}f)+CD({}^{CD}f)\ . \qquad (1.4)$$

Both product molecules can exhibit internal excitation (${}^{AB}f$, ${}^{CD}f$) in contrast to reaction (1.2). Indeed, both product molecules of process (1.3) are chemically identical, but with the use of the isotopic labeling technique it is possible to determine exactly the origin of a given hydroxyl molecule. In a model of a direct reaction (in contrast to complex formation), it it possible to characterize the original OH bond in a reactant H_2O molecule as well as the newly formed OH product partner.

Due to the very detailed experimental data obtained from a previous study of the products' internal distributions[8] it was possible to calculate for the first time, microscopic reaction probabilities for two coincident product molecules emerging from a chemical reaction.[10] We have now extended this study of four-body dynamics to the reaction

$$^{16}O(^1D)+D_1\ ^{18}O\rightarrow {}^{16}OD(^{16}f)+{}^{18}OD(^{18}f)\ . \qquad (1.5)$$

One result of the reaction of $O+H_2O$ is that the process is very direct and can be described by a simple abstraction mechanism. The mass of the "jumping" hydrogen atom is doubled in process (1.5) so that the dynamical

[a)] Alexander von Humbolt U. S. Senior Scientist on Sabbattical from the Department of Chemistry, University of Utah, Salt Lake City, UT 84112.

 0021-9606/83/105993-09$02.10 © 1983 American Institute of Physics

Downloaded 16 Aug 2004 to 129.67.71.67. Redistribution subject to AIP license or copyright, see http://jcp.aip.org/jcp/copyright.jsp

restriction for the stripped atom can be studied and the reactant mass dependence on the energy partitioning of the products can be ascertained. Furthermore, more internal quantum states of the OD molecule can be populated than for the OH radical because of the smaller vibrational quantum frequency. This factor should have an influence on the microscopic reaction probability for two coincident product molecules, since for a given molecule the coincident partner molecule is in principle more free to populate different internal quantum states.

EXPERIMENTAL

The detailed study of the energy partitioning in an elementary reactive collision requires that the products be observed in their nascent distribution, i.e., under collision free conditions. In the case of very reactive species such as reaction (1.5), the pump and probe technique is a practicable procedure, if the production of $O(^1D)$ and the observation of the OD product molecules occur on a time scale which is not longer than the collision time of the species. The use of the pump and probe technique in contrast to molecular beams has the advantage that, besides the simpler experimental arrangement, the observed number density $N(f)$ in a specific quantum state f is directly proportional to the production probability $P(f)$, assuming that all product molecules $N(f)$ in the quantum state f are observed. In the case of molecular beams, the probability $P(f)$ depends additionally on the translational energy $E_T(f)$ of the product molecules. However, it is usually difficult, if not impossible, to obtain the translational energy $E_T(f)$ in each *individual* elementary reactive collision.[11]

Our experimental setup shown in Fig. 1 consists of the pump and probe laser system, the gas handling system, and the detection system. The $O(^1D)$ atoms are formed by pulse photolysis of ozone in a $D_2{}^{18}O$–$^{16}O_3$ mixture with the fourth harmonic of a Nd: YAG laser (DCR of quanta ray) at 266 nm, near the absorption maximum of ozone. The dissociation process:

$$^{16}O_3 + h\nu(266\text{ nm}) \rightarrow {}^{16}O(^1D) + {}^{16}O_2(^1\Delta_g) \qquad (2.1)$$

has been previously analyzed in detail[12–17] and has a quantum yield of $\Phi[O(^1D)] \simeq 0.9$.[15–17] The other dissociation channel yields an oxygen atom in the ground state and $\Phi[O(^3P)] \simeq 0.1$. The $O(^1D)$ atoms are formed with a high excess of translational energy, as shown by the molecular beam study of Lee and co-workers.[16] The $O(^1D)$ atoms react very fast[18] with the isotopically labeled $D_2{}^{18}O$ molecules to form $^{16}OD(^{16}f)$ and $^{18}OD(^{18}f)$ in each reactive collision:

$$^{16}O(^1D) + D_2{}^{18}O \rightarrow {}^{16}OD(^{16}f) + {}^{18}OD(^{18}f)\ . \qquad (2.2)$$

The number densities, i.e., the reaction probabilities $P(^{16}f)$ and $P(^{18}f)$ are probed by a tunable pulsed dye laser (quantel TDL III). The radiation of the second harmonic of the Nd: YAD laser is used to pump this dye laser. In order to correlate the $O(^1D)$ production time exactly with the $OD(f)$ probe time, the fourth harmonic photolysis pulse as well as the second harmonic pump pulse of the dye laser, are extracted from the same laser system simultaneously. The radiation of the second harmonic of the YAG laser is optically delayed relative to the fourth harmonic at a delay time of 10 ns to allow the $O(^1D)$ atom to react with D_2O. Hence the two laser pulses are exactly correlated to each other in time and jitter free operation was obtained, even below 10 ns.

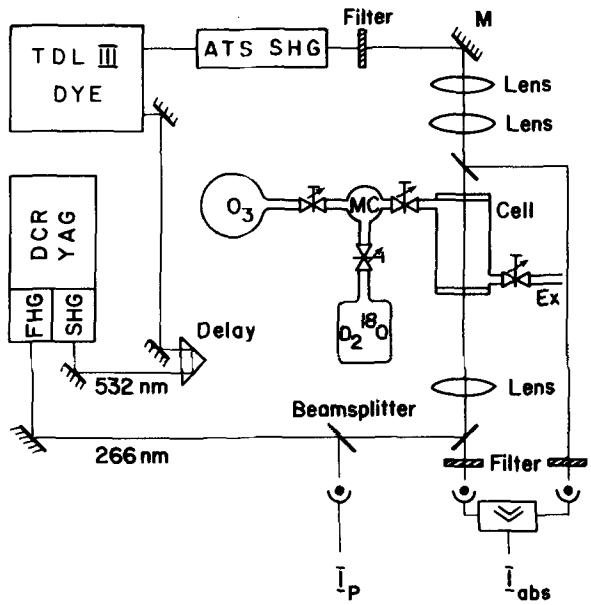

FIG. 1. Schematic diagrams of the experimental setup to study the reaction $^{16}O(^1D) + D_2{}^{18}O + {}^{16}OD + {}^{18}OD$. The $O(^1D)$ atoms are produced by photolyzing ozone with radiation of the fourth harmonic (FHG) of a Nd:YAG laser (DCR YAG) at 266 nm. Both product molecules are probed with a tunable frequency doubled dye laser (TDL III DYE), which is pumped by the radiation of the second harmonic (SHG) of the Nd:YAG laser at 532 nm. The gases $^{16}O_3$ and $D_2{}^{18}O$ are flowing through the sample cell. Pressure and flow rates are controlled by capacity manometers and needle valves.

The gases were pumped through the reaction cell at constant pressures of 2 Torr for ozone and 10 Torr for $D_2{}^{18}O$ at room temperature. The flow rates were adjusted by needle valves, and the pressures were controlled by means of capacitance manometers (MKB). Water samples were 99% pure $D_2{}^{18}O$. The ozone was prepared by flowing gaseous O_2 through an electrical discharge and trapped into a U trap filled with silica gel cooled at $-60\,^\circ$C. For a typical experimental run, the O_3 was distilled from the U trap into a large ($\sim 6\ \ell$) bulb from which it was flowed via a needle valve into the mixing chamber (MC).

The detection of the nascent OD radicals was performed by resonance absorption of the $\tilde{A}\,^2\Sigma - \tilde{X}\,^2\Pi$ transition in the region above 300 nm.[19–21] The fundamental wavelength region above 600 nm (Rd B) was frequency doubled by an INRAD "auto tracking system" (ATS). This ATS automatically tunes the crystal for second harmonic generation as a function of the incoming radiation. Beam displacement was compensated automatically by a quartz flat. The probe dye laser beam is split into two beams, with one of them bypassing the cell to compensate for intensity fluctuation. The other beam, which passes through the cell, is directed to a special dielectric mirror, which has a high transmission for radiation above 300 nm but a high reflection

Downloaded 16 Aug 2004 to 129.67.71.67. Redistribution subject to AIP license or copyright, see http://jcp.aip.org/jcp/copyright.jsp

(> 99%) for the photolyzing radiation of the fourth harmonic of the YAG laser at 266 nm. With the aid of this mirror, both beams, the probe beam of the dye laser and the pump beam of the YAG laser, could be perfectly collinearly aligned to each other so that the dye beam always probed a homogeneous reaction region. The signals were monitored by UV diodes, stored and averaged by a boxcar integrator (PAR, model 162), and displayed on a recorder. The probe dye laser has two gratings, which in turn reduced the bandwidth to < 3 GHz (determined with the aid of an external etalon). The Doppler width of the OD transitions at room temperature is ~3 GHz, thus, the absorption line profiles of the (hot) OD species produced in the reaction were measured and the temperature of the velocity distribution of the products can be determined.

The locations of the absorption lines, as well as the transition probabilities for determining $P(f)$ were taken from the literature.[20,22] The values for the energy levels for ^{16}OD were taken from Ref. 20. In this analysis we used for ^{18}OD the same energy levels as for ^{16}OD, because the small energy difference does not cause any serious effect. The spectroscopic terminology and notation of Dieke and Crosswhite is used.[19] An additional result of the treatment of the spectroscopic data is a set of molecular constants and energy levels for the upper and lower electronic states of the ^{18}OD molecule.[21]

If we compare the reaction of $O(^1D)$ with D_2O and the reaction of $O(^1D)$ with H_2O, then it is obvious that more quantum states of OD will be populated in contrast to the OH molecule for the same excess energy. As a consequence, the relative population number of one OD quantum state will be less and the absorption will decrease. Therefore, the measured peak heights of a scan over the individual absorption lines show an uncertainty of 25%. In unfavorable cases, i.e., for extremely small absorptions and isolated lines between vibrational bands, the uncertainty can be ~40%. However, the values are derived from several experimental data and therefore the standard error is distinctly smaller.

The observed reaction probabilities are presented in their original form, without smoothing or any numerical reduction of the relaxation phenomena.[23] Only the data which represent the same quantum state (e.g., the R and P lines) were averaged to reduce the standard error.

RESULTS

The total excess energy E which is available to the product molecules is determined by the translational energy $E_t(O, D_2O)$ of the reactants, the internal reactant energy $E_{in}(D_2O)$, and the ground-state to ground-state exoergicity ΔE:

$$E = E_t(O, D_2O) + E_{in}(D_2O) + \Delta E \ , \tag{3.1}$$

$D_2{}^{18}O$ and O_3 are at thermal equilibrium, $T = 300$ K,

$$E_{in}(D_2O) = E_{vib}(D_2O) + E_{rot}(D_2O) \simeq 3.7 \text{ kJ mol}^{-1} \ . \tag{3.2}$$

The translational energy $E_t(O, D_2O)$ is given by Eq. (3.3) (see also Appendix A of Ref. 10):

$$E_t = \mu/2\,[3RT/M_{D_2O} + 3RT/M_{O_3} + 2E_t(O, O_2)\,\mu_{O,O_2}/m_O^2] \ , \tag{3.3}$$

where μ is the reduced mass for the ^{16}O–$D_2{}^{18}O$ system. $E_t(O, O_2)$ and μ_{O,O_2} are the translational energy and reduced mass of the dissociated $^{16}O + {}^{16}O_2$, respectively. The nonthermal distribution of $E_t(O, O_2)$ has been determined experimentally.[16] Inserting the average value of $\bar{E}_t(O, O_2) = 54.4$ kJ mol^{-1} in Eq. (3.3), one obtains for the translational energy of the reactants:

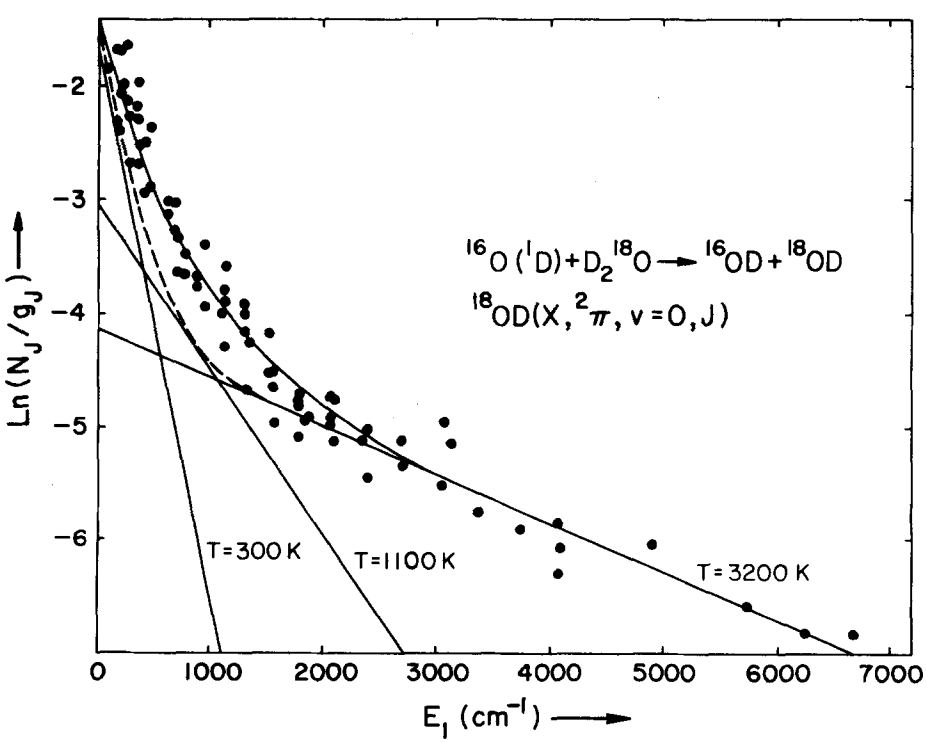

FIG. 2. Distribution of produced ^{18}OD arising from the reaction $^{16}O(^1D) + D_2{}^{18}O \rightarrow {}^{16}OD + {}^{18}OD$ in the rotational states of $^2\Pi_{3/2,1/2}(v'' = 0)$ for both Λ levels. The plot is the logarithm of the population number N_J which is proportional to the reaction probability, divided by the degeneracy $g_J = 2J + 1$ vs the internal energy so that the slope is $-1/kT_v$. The values for T_v are shown. The dashed line is the superposition of the distributions for the $T = 300$ K and $T = 3200$ K. The solid line is obtained additionally a $T = 1100$ K distribution being included. Experimental conditions: $P_{D_2O} = 10$ Torr, $P_{O_3} = 2$ Torr delay time 10 ns. The same conditions obtained for Figs. 3–6.

Downloaded 16 Aug 2004 to 129.67.71.67. Redistribution subject to AIP license or copyright, see http://jcp.aip.org/jcp/copyright.jsp

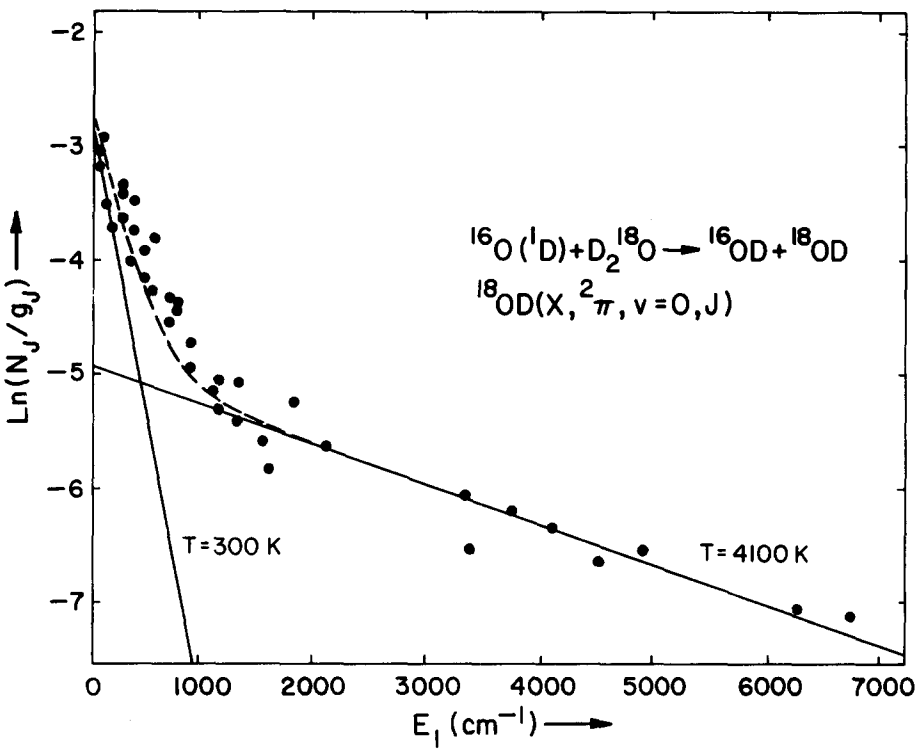

FIG. 3. Distribution of produced ^{16}OD in the rotational states of $^2\Pi_{3/2,1/2}$ ($v''=0$) for both Λ levels. The plot is $\ln[N_J/(2J+1)]$ vs the internal energy so that the slope is $-1/kT_v$. The dashed line is the superposition of the two disbributions for $T=300$ K and $T=4100$ K. Experimental conditions are the same obtained for Fig. 2.

$$E_t(O, D_2O) = 23.2 \text{ kJ mol}^{-1} . \quad (3.4)$$

With the value of $\Delta E = 117$ kJ mol^{-1},[24] the total excess energy

$$E = 139.9 \text{ kJ mol}^{-1} \quad (3.5)$$

is available to the reactants.

Rotational distributions

The rotational state distribution $P(^{16}J)$ and $P(^{18}J)$ for ^{16}OD and ^{18}OD in the different vibrational manifolds is quite broad. The experimental results for $^{18}OD(^{18}f)$ (which in the case of a direct reaction, represents the original bond which existed in $D\,^{18}O-D$) are shown in Fig. 2. Here, ^{18}f represents $^{18}f = (^{18}v=0, {}^{18}J, {}^{18}\Lambda, {}^{18}\Omega)$, Λ stands for the different lambda components, and Ω for the two spin states. The x axis represents the internal energy $E_I = E_{vib} + E_{rot}$ in wave numbers of the product molecule and the y axis represents the natural logarithm of the observed population in a quantum state divided by the degeneracy $g_J = 2J+1$ of this state. It should be noted that the population shown is proportional to the reaction probability $N_J \sim P(J, \Omega, \Lambda, v=0)$. Thus, no averaging procedure has been done for the different lambda or spin components.

In this figure are also included straight lines, which represent Boltzmann-like distributions. These distributions are characterized by a temperature parameter T_v. The value of T_v is also included in Fig. 2. For higher rotational energies the state distribution can be described by a single line. Figure 3 shows the distribution of $^{16}OD(^{16}f)$, $^{16}f = (v=0, J, \Lambda, \Omega)$. The plot is also $\ln[N_J/(2J+1)]$ vs the internal energy so that the slope is $-1/kT_v$. For high rotational energies this distribution is characterized by $T_{v=0} \simeq 4100$ K.

In order to obtain a better view over the relative percentage of both product molecules in each J level, Fig. 4 shows the relative fraction of $^{18}OD(^2\Pi, v'', J'')$ radicals in different rotational levels of the same vibrational manifold (filled circles for $v''=0$). It is seen that the fractional contribution $\Phi(E_I|v''=0)$ of $^{18}OD(^2\Pi, J'', v''=0)$ is higher in lower rotational states ($\Phi > 0.8$) and decreases for higher ones. However, even in the very high rotational levels, the percentage is not less than 50%.

The rotational distribution for ^{16}OD in the first vibrational level is shown in Fig. 5. As before, we can describe this distribution by a parameter $T_{v=1} = 2000$ K but the value is reduced in comparison with the vibrationless state. No temperature distribution for ^{18}OD is specified, because the total amount of ^{18}OD decreases drastically in this vibrational state. As we can see from Fig. 4 (filled squares) the fraction $\Phi(E_I|v''=1)$ of ^{18}OD in $v''=1$ for each rotational state is reduced in contrast to $v''=0$. Only 25% of all molecules produced in $v''=1$ are ^{18}OD radicals.

In even higher vibrational states it is difficult to detect the distribution of all product molecules due to the reduced transition probabilities and the smaller amount of radicals which populate these levels. The data obtained for higher rovibrational levels are insufficient to justify the plot of a rotational distribution, but we can conclude the following: the original bond ^{18}OD is mainly produced in $v''=0$ and only a very small part can be found in $v''=1$, whereas the newly formed bond ^{16}OD is distributed over the vibrational levels. The rotation shows a broad distribution for ^{16}OD and ^{18}OD. With increasing vibrational excitation, the rotational distribution attains a converging limit before reaching the exoergetic limit.

Downloaded 16 Aug 2004 to 129.67.71.67. Redistribution subject to AIP license or copyright, see http://jcp.aip.org/jcp/copyright.jsp

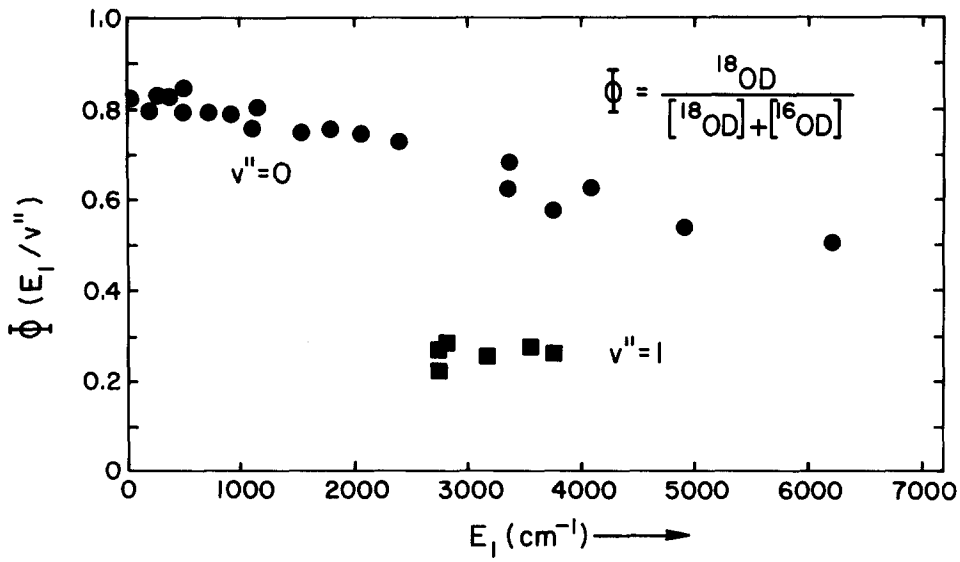

FIG. 4. Ratio of ^{18}OD to the total amount of produced OD radicals $[^{16}OD(^{16}J) + ^{18}OD(^{18}J)]$ in a specific rotational state vs the internal energy. Filled circles represent the vibrationless state $v'' = 0$, filled squares stand for the first vibrational state. No ^{18}OD in $v'' \geq 2$ could be found. The experimental conditions are the same obtained for Fig. 2.

Vibrational distribution

The vibrational distributions $^{16}P(v)$ and $^{18}P(v)$ are obtained by summation of the population of all quantum states belonging to the same vibrational manifold:

$$P(v) = \sum_J \sum_\Lambda \sum_\Omega P(J, \Lambda, \Omega, v)\ . \tag{3.6}$$

These vibrational distributions vs the vibrational energy are shown in Fig. 6. The ^{18}OD molecules are formed nearly exclusively (92%) in the vibrationless state. The remaining fraction of 8% is produced in the first vibrational state.

A quite different distribution is found for ^{16}OD (the newly formed bond) which is distributed over all available vibrational states. The total vibrational energy is mainly channeled into the new bond, while the original bond remains vibrationally cold.

The mean vibrational excitation $\langle E_v \rangle$,

$$\langle E_v \rangle = \sum_v \sum_J \sum_\Lambda \sum_\Omega P(v, J, \Lambda, \Omega) E_v \tag{3.7}$$

$$= \sum_v E_v P(v) \tag{3.8}$$

and the mean rotational excitation $\langle E_r \rangle$

$$\langle E_r \rangle = \sum_v \sum_J \sum_\Lambda \sum_\Omega P(v, J, \Lambda, \Omega) E_r \tag{3.9}$$

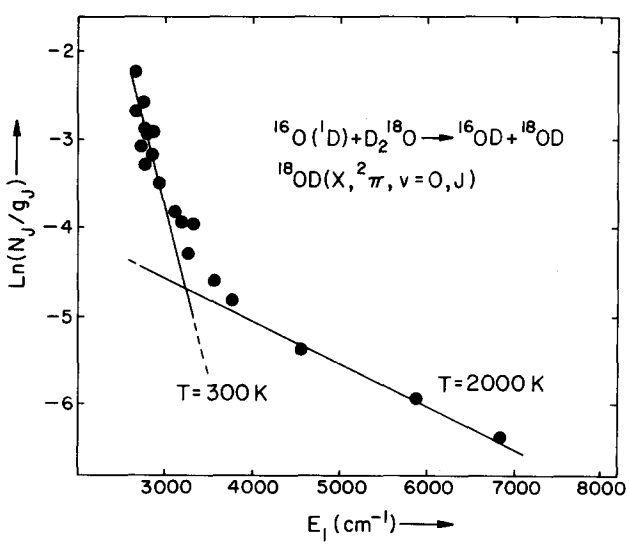

FIG. 5. Distribution of produced ^{16}OD in the rotational states of $^2\Pi_{3/2,1/2}$ ($v'' = 1$) for both Λ levels. The plot is $\ln[N_J/(2J+1)]$ vs the internal energy E_I so that the slope is $-1/kT_v$. The dashed line is the superposition of the two distribution for $T = 300$ K and $T = 2000$ K. Experimental conditions are the same obtained for Fig. 2.

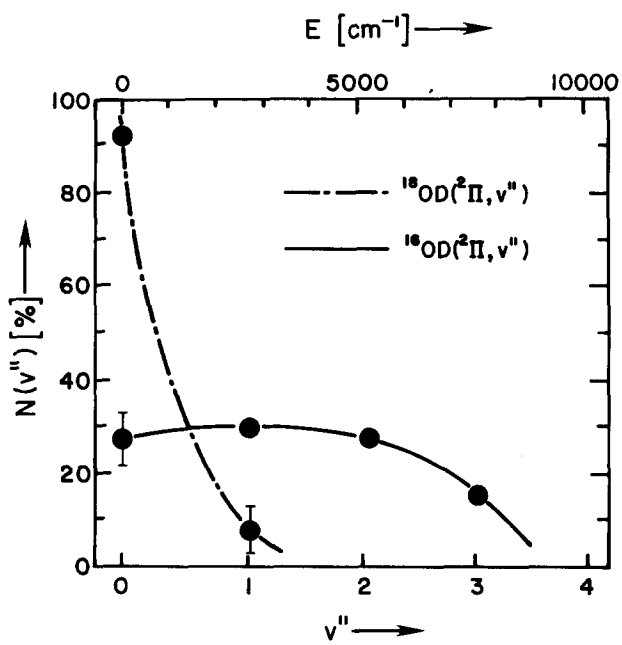

FIG. 6. Distribution of $^{18}OD(^2\Pi, v'')$ (—·—·) and $^{16}OD(^2\Pi, v'')$ (—) in the vibrational states of the electronic ground state. The plot shows the population number, which is proportional to the reaction probability for the vibrational states, vs the energy E (cm^{-1}) or the quantum number v''. Experimental conditions are the same obtained for Fig. 2.

Downloaded 16 Aug 2004 to 129.67.71.67. Redistribution subject to AIP license or copyright, see http://jcp.aip.org/jcp/copyright.jsp

TABLE I. Mean vibrational and rotational excitation for the reactions of $^{16}O + D_2\,^{18}O$ and $^{16}O + H_2\,^{18}O$.

	$^{16}O(^1D) + D_2\,^{18}O$		$^{16}O(^1D) + H_2\,^{18}O$	
	^{16}OD	^{18}OD	^{16}OH	^{18}OH
$\langle E_v \rangle$	41.1	2.4	31.4	3.4
$\langle E_r \rangle$	16.7	15.9	16.0	15.7
$\langle E_I \rangle$	76.1		66.5	
E	139.9		147.5	

$\langle E_I \rangle$ is the mean internal excitation of the product molecules for the available energy E. All units are kJ/mol.

are summarized in Table I. Also included in Table I are the mean vibrational and rotational excitation for the reaction of $^{16}O(^1D) + H_2\,^{18}O$. As expected, $\langle {}^{16}E_v \rangle$ is quite different from $\langle {}^{18}E_v \rangle$, whereas the mean rotational excitation is the same for ^{16}OD and ^{18}OD:

$$\langle {}^{16}E_r \rangle \simeq \langle {}^{18}E_r \rangle \ . \tag{3.10}$$

The electronic ground state of the OD radical is split into two spin components which are both Λ doubled. Each of these four components can be spectroscopically resolved with the experimental setup used, and the reaction probabilities for these states are obtained. The experimental data show that within the error limits, the ^{16}OD and ^{18}OD product molecules are distributed statistically between their two Λ components and between the two possible spin states. For this reason, all measured population numbers are included in Figs. 2, 3, and 5, and no special representation for the spin or Λ components is necessary.

DISCUSSION

The reaction of metastable oxygen atoms in the (^1D) state with $D_2\,^{18}O$ proceeds with a gas kinetic rate and a small activation energy which is expected to have no influence on the reaction rate as observed for different $O(^1D)$ translational velocities.[18] Therefore, the reaction is expected to proceed on a long range attractive potential surface. Following the simple "rules" of Polanyi[25] then early (late) downhill potential energies lead to vibrationally excited (nonexcited) product molecules. The ^{16}OD has a high degree of vibrational excitation and the potential energy surface is probably of the "early-downhill" character.

With the help of simple mass relations, Smith[26] has shown that the maximum of vibrational energy for AB in the reaction

$$A + BCD \rightarrow AB + CD \tag{4.1}$$

in a colinear arrangement is given by

$$\langle {}^{AB}E_v \rangle_m = E \cdot \sin^2 \beta \ , \tag{4.2}$$

where E is the total available energy to the products and β depends only on the masses of the involved atoms:

$$\tan \beta = M m_B / m_A (m_C + m_D) \ , \tag{4.3}$$

and

$$M = m_A + m_B + m_C + m_D \ . \tag{4.4}$$

The results for $\langle {}^{16}E_v \rangle_m$ and $\langle {}^{18}E_v \rangle_m$ are summarized in Table II. The analysis of Smith shows an increase of the mean vibrational excitation when the mass of the jumping atom is increased. The experimental results qualitatively confirm this trend while for a quantitative analysis the consideration of simple mass relations given in Eqs. (4.2)–(4.4) are too simple.

The vibrational excitation of the ^{16}OD radical is even higher than expected on prior grounds of the information theory.[27] Without special consideration of the origin of the two product molecules the prior probability $P^\circ(^{16}f, {}^{18}f)$ is given by

$$P^\circ(^{16}f, {}^{18}f) \propto (2\,{}^{16}J + 1)(2\,{}^{18}J + 1)\, E_t^{1/2} \ , \tag{4.5}$$

where $E_t^{1/2}$ measures the translational degeneracy.

$$E_t = E - E(^{16}v) - E(^{18}v) - E(^{16}J) - E(^{18}J) \ . \tag{4.6}$$

The prior probability $P^\circ(^{16}v)$ is then given by the summation over all other quantum states until the maximum available energy E is reached

$$P^\circ(^{16}v) \propto \sum_{^{16}J} \sum_{^{18}J} \sum_{^{18}v} (2\,{}^{16}J + 1)(2\,{}^{18}J + 1)\, E_t^{1/2} \ . \tag{4.7}$$

The results of such an analysis are summarized in the first column of Table II. As can be seen the OD should exhibit a broader vibrational excitation than the OH, which can be verified by the experiment. In a manner similar to OH, the OD excitation in the vibrational excited states is much higher than predicted on prior grounds.

The distribution of ^{18}OD over the different vibrational levels is described by the same prior $P^\circ(^{18}v)$. (The small differences in the energy levels for ^{16}OD and ^{18}OD are negligible.) Thus, the ^{18}OD is vibrationally much colder than on prior grounds. It is like a "spectator"

TABLE II. Vibrational distribution for ^{16}OD, ^{18}OD and ^{16}OH, ^{18}OH assuming a prior distribution $P^\circ(v)$ and a prior distribution for conicident pairs $P^\circ_{cp}(v)$ in comparison with the experimental data (units are percent). Also shown are the average vibrational excitations $\langle E_v \rangle$ (in kJ/mol) for these prior distributions and $\langle E_v \rangle_m$, which is predicted for a simple mass analysis (Ref. 26). If not otherwise noted, the values refer to both isotopic species.

	$^{16}O + D_2\,^{18}O \rightarrow {}^{16}OD + {}^{18}OD$				$^{16}O + H_2\,^{18}O \rightarrow {}^{16}OH + {}^{18}OH$		
v	0	1	2	3	0	1	2
$P^\circ(v)$	58	28	11	3	69	25	6
$P^\circ_{cp}(v)$	49	29	15	6	59	29	11
$^{16}P_{expt}(v)$	27	29	28	16	46	36	18
$^{18}P_{expt}(v)$	92	8	0	0	92	8	0
$\langle E_v \rangle^\circ$		18.3				15.8	
$\langle E_v \rangle^\circ_{cp}$		23.9				21.5	
$\langle {}^{16}E_v \rangle_m$		27.7				15.5	
$\langle {}^{18}E_v \rangle_m$		0				0	

Downloaded 16 Aug 2004 to 129.67.71.67. Redistribution subject to AIP license or copyright, see http://jcp.aip.org/jcp/copyright.jsp

during the reactive collision, which means that the original ^{18}OD bond in $D-^{18}O-D$ is conserved. In contrast to the quite specific and different distributions of ^{16}OD and ^{18}OD radicals over the vibrational levels is the rotational excitation of the product molecules.

Before discussing the nascent rotational distribution in the vibrational levels we must consider the influence of rotational relaxation. The delay time between the pump pulse of the fourth harmonic of the Nd: YAG laser and probe pulse of the doubled dye laser is adjusted to 10 ns for a total pressure of 12 Torr. Thus, on the average, the observed product molecules should have undergone less than one gas kinetic collision. Furthermore, the energy spacing between the rotational levels is relatively large for OH and OD, so that more than one collision should be necessary to relax the rotational distribution. However, in a detailed study of the rotational relaxation phenomena of OH,[23] it was shown that each collision produced very efficient rotational relaxation and that the relaxed distribution could be characterized by a Boltzmann distribution with a temperature parameter of ~300 K. If we take into account such relaxation phenomena in this study, then the population numbers of the observed rotational distribution should be describable by two straight lines similar in form to Figs. 2, 3, and 5. The dashed line (---) in these figures is the sum of both Boltzmann distributions.

As can be seen, this new description is fully valid for ^{16}OD in the first vibrational level, less for ^{16}OD in $v'' = 0$, but absolutely not for ^{18}OD in $v'' = 0$. The rotational relaxation should not vary in such a manner between two vibrational levels. Therefore, we cannot describe the nascent rotational distribution by one single Boltzmann parameter. However, an explanation for the rotational distribution is straightforward if microscopic probabilities for two coincident product molecules are taken into account.

In a previous paper[10] for the reaction (1.3), $P(^{16}f, ^{18}f)$ was determined, the *joint* probability of simultaneously observing $^{16}OH(^{16}f)$ *and* $^{18}OH(^{18}f)$. This joint probability $P(^{16}f, ^{18}f)$ provides more detailed information about process (1.3) than $P(^{16}f)$ and $P(^{18}f)$, because the internal distribution of one radical is only the sum of $P(^{16}f, ^{18}f)$ over all internal quantum states of the other radical. As an example, the experimental observable probability $P_{exp}(^{16}v)$ for detecting $^{16}OD(^{16}v)$ in the vibrational level ^{16}v is given by

$$P_{exp}(^{16}v) = \sum_{^{18}v=0}^{4-^{16}v} P(^{16}v, ^{18}v) , \quad 0 \leq {}^{16}v \leq 4 \tag{4.8}$$

and similarly for $^{18}OD(^{18}v)$:

$$P_{exp}(^{18}v) = \sum_{^{16}v=0}^{4-^{18}v} P(^{16}v, ^{18}v) , \quad 0 \leq {}^{18}v \leq 4 . \tag{4.9}$$

For the system $^{16}O + H_2\,^{18}O$, the joint vibrational and rotational probabilities were obtained. The important conclusion from that paper is the following: Either the newly formed radical ^{16}OH is vibrationally excited in a reactive collision, or, to a much smaller extent, the "old" radical ^{18}OH, but not both simultaneously.

From that conclusion, it follows that the observed distributions for $^{18}OH(^{18}v = 0)$ and $^{16}OH(^{16}v = 0)$ actually arise from the *superpositions* of joint reaction probabilities with the partner molecules each in several vibrational levels, respectively. In contrast the $^{18}OH(^{18}v = 1)$, $^{16}OH(^{16}v = 1)$, and $^{16}OH(^{16}v = 2)$ are characterized by *single* parameters.

If we apply this conclusion to the $^{16}O + D_2\,^{18}O$ system, then the nascent distribution of $^{16}OD(^{16}v = 1)$ should be "clean", i.e., it should be describable by a single parameter. Indeed, this is valid, if we neglect the rotational relaxation.

The distributions of $^{16}OD(^{16}v = 0)$ and $^{18}OD(^{18}v = 0)$ are superpositions of joint reaction probabilities. The fact that ^{18}OD is nearly vibrationally cold only causes the small amount of $^{18}OD(^{18}v = 1)$ to be added to the distributions of $^{16}OD(^{16}v = 0)$. Therefore the distribution of $^{16}OD(^{16}v = 0)$ can be nearly described by a single parameter. The data points are located slightly above the dashed line of Fig. 3 indicating the partner molecule in $^{18}v = 1$.

The newly formed bond ^{16}OD is spread over the vibrational levels. Therefore the distribution of $^{18}OD(^{18}v = 0)$ should show the strongest deviation from the dashed line shown in Fig. 2. Unfortunately, the observed intensity of the rotational distribution for $^{16}v \geq 2$ is too weak to determine exact superposition of different reaction probabilities. However, a mean rotational distribution ($T = 1100$ K) for the vibrational excited states is assumed, and the total amount of ^{16}OD in these vibrational levels is considered. With this additional rotational distribution, the population numbers of $^{18}OD(^{18}v = 0)$ in the vibrationless state can be described as shown by the pointed line indicated in Fig. 2.

The total angular momentum J_t, which is a conserved quantity for reactants and products, is determined by the rotational (J) and initial orbital angular momentum (L_t):

$$J_t = J_{O(^1D)} + J_{D_2O} + L_t = {}^{16}J + {}^{18}J + L_f , \tag{4.10}$$

$J_{O(^1D)} = 2\hbar$ and $J_{D_2O} \simeq 4\hbar$ at room temperature $T = 300$ K. The average orbital angular momentum L_t can be estimated classically from the relation

$$L_t = \tfrac{1}{2} L_{max} = \tfrac{1}{2} \mu v s , \tag{4.11}$$

with μ, v, and s representing the reduced mass $[O(^1D) - D_2\,^{18}O]$, the average velocity, and the maximum impact parameter of the reactants. For the rate constant k, we use the relation

$$k = v\sigma = \pi v s^2 \tag{4.12}$$

and for v the relation

$$v = \sqrt{2E_t/\mu} . \tag{4.13}$$

Inserting Eqs. (4.13) and (4.12) into Eq. (4.11), we obtain for the orbital angular momentum

$$L_t = \left(\frac{k^2 \mu^3 E_t}{8\pi^2}\right)^{1/4} , \tag{4.14}$$

with the data for the reaction $O + D_2O$ we obtain the final result:

Downloaded 16 Aug 2004 to 129.67.71.67. Redistribution subject to AIP license or copyright, see http://jcp.aip.org/jcp/copyright.jsp

$$L_t = 2.0\times10^{-33}\ Js \simeq 28\hbar\ . \tag{4.15}$$

The maximum total angular momentum is then

$$J_t \simeq 34\hbar\ . \tag{4.16}$$

The final angular momentum L_f can be estimated from the final translational energy $\langle E_T\rangle = E - \langle E_I\rangle$ implied in Table I. Equation (4.14) gives the value $L_f \simeq 35\hbar$, which suggests the relation,

$$J_t \simeq L_f\ . \tag{4.17}$$

From this model assumption it follows[28] when we introduce Eq. (4.17) into Eq. (4.10) both product molecules have the *same* rotational orbital momentum, but rotate with opposite angular velocity. A consequence is that ^{16}OD and ^{18}OD have the same average rotational excitation $\langle E_r\rangle$, which is confirmed by the experimental data [Eq. (3.10)].

An additional consequence of the "constraint" $^{18}J = -{}^{16}J$ is that for the production of coincident hydroxyl radical pairs, the degeneracy is only $(2J+1)$, which changes the prior probability for coincident events. Now the prior probability P°_{cp} is given by

$$P^\circ_{cp}(^{16}f, {}^{18}f) \propto (2J+1)\, E_t^{1/2} \tag{4.18}$$

and a different prediction for the vibrational distribution is made. As shown in Table II, $P^\circ_{cp}(v)$ has a broader vibrational distribution which is a better fit to the experimental data.

Another interesting point is the dependence of the orbital angular momentum on translational energy. The reaction should not be very sensitive to a change in translational energy if the total reaction rate constant is not. This is because L_t depends only on the fourth root of E_t [Eq. (4.14)]. In a blank study of the influence of the translational energy on the energy partitioning in the reaction $O(^1D) + H_2O$, it was shown[23] that translationally hot and cold $O(^1D)$ atoms do not change the internal state distribution of the product radicals.

CONCLUSIONS

The vibrational energy partitioning of reaction (1.5) is very specific (Fig. 6) and definitely deviates from prior expectations. The vibrational excitation is preferably channeled into the new ^{16}OD bond in contrast to the rotational excitation. Both product radicals rotate with the same velocity but in opposite directions. The internal angular momentum distributions of the excited vibrational manifolds of one product molecule arise from collisions in which the partner molecule is in its vibrational ground state. Conversely, the internal distribution of vibrationally cold radicals arises from reactive collisions where the partner molecule is excited over several vibrational levels. Therefore, the distributions of vibrationally cold product molecules have to be described by more than one parameter (Fig. 2). The distribution of the isotopically labeled molecules reflect a direct type of reaction mechanism, in contrast to a long-lived collision complex or compound mechanism.[29] The reaction must proceed on a time scale which does not allow for efficient energy transfer into all available phase space. As a consequence, the reaction time should be determined by the pass-by time of the $^{16}O(^1D)$ atom.

ACKNOWLEDGMENTS

We should like to thank the Deutsche Forschungsgemeinschafft for financial support. W. A. G. extends sincere appreciation to the Alexander von Humboldt Foundation for the support of a U. S. Senior Scientist award during which this work was performed and the Department of Energy for partial support of this project through Contract No. DEAC0278ER046905.

[1] I. W. M. Smith, *Kinetics and Dynamics of Elementary Gas Reactions* (Butterworths, London, 1980).
[2] I. Carrington and J. C. Polanyi, Int. Rev. Sci. **9** (1972).
[3] D. H. Maylotte, J. C. Polanyi, and U. B. Woodall, J. Chem. Phys. **57**, 1547 (1972).
[4] J. G. Moehlmann and J. D. McDonald, J. Chem. Phys. **59**, 59 (1973).
[5] R. Engleman, J. Am. Chem. Soc. **87**, 4193 (1965).
[6] K. H. Gericke and F. J. Comes, Chem. Phys. Lett. **74**, 63 (1980).
[7] J. E. Butler, L. D. Talley, G. K. Smith, and N. L. Lin, J. Chem. Phys. **74**, 4501 (1981).
[8] K. H. Gericke, F. J. Comes, and R. D. Levine, J. Chem. Phys. **74**, 6106 (1981).
[9] M. D. Rodgers, K. Asaind, and D. D. Davis, Chem. Phys. Lett. **78**, 246 (1981).
[10] F. J. Comes, K. H. Gericke, and J. Manz, J. Chem. Phys. **75**, 2853 (1981).
[11] A way out is shown by J. L. Kinsey, J. Chem. Phys. **66**, 2560 (1977); E. J. Murphy, L. H. Brophy, G. S. Arnold, L. Dimpfl, and J. L. Kinsey, *ibid.* **70**, 5910 (1979). J. A. Serri, J. L. Kinsey, and D. E. Pritchard, *ibid.* **75**, 663 (1981).
[12] J. W. Simons, R. J. Paur, H. A. Webster III, and E. J. Bair, J. Chem. Phys. **59**, 1203 (1973).
[13] I. Arnold, F. J. Comes, and G. K. Moortgat, Chem. Phys. **24**, 211 (1977).
[14] D. L. Baulch, R. A. Cox, R. F. Hampson, Jr., J. A. Kerr, J. Troe, and X. Watson, J. Phys. Chem. Ref. Data **9**, 295 (1980).
[15] C. E. Fairchild, E. J. Stone, and G. M. Lawrence, J. Chem. Phys. **69**, 3632 (1978).
[16] R. K. Sparks, L. R. Carlson, K. Shobatake, M. L. Kowalczyk, and Y. T. Lee, J. Chem. Phys. **72**, 1401 (1980).
[17] J. L. Brock and R. T. Watson, Chem. Phys. Lett. **71**, 371 (1980).
[18] K. H. Gericke and F. J. Comes, Chem. Phys. Lett. **81**, 2186 (1981). This paper gives reference to all previous measurements of the total rate coefficient of the reaction $O(^1D) + H_2O \rightarrow 2$ OH.
[19] G. H. Dieke and H. M. Crosswhite, J. Quant. Spectrosc. Radiat. Transfer **2**, 97 (1961).
[20] M. A. Clyne, J. A. Coxon, and A. R. Woon Fatt, J. Mol. Spectrosc. **46**, 146 (1973).
[21] M. Nuβ, K.-H. Gericke, F. J. Comes, and W. A. Guillory J. Quant. Spectrosc. Radiat. Transfer (in press).
[22] W. L. Dimpfl and J. L. Kinsey, J. Quant. Spectrosc. Radiat. Transfer **21**, 233 (1979); J. L. Kinsey (private communication).
[23] K. H. Gericke and F. J. Comes, Chem. Phys. **65**, 113 (1982).
[24] J. C. Tully, J. Chem. Phys. **62**, 1893 (1975).
[25] J. C. Polanyi and J. L. Schreiber, *Physical Chemistry an Advanced Treatise* (Academic, New York, 1974), Vol. VIA; R. D. Levine and R. B. Bernstein, *Molecular Reaction Dy-*

Downloaded 16 Aug 2004 to 129.67.71.67. Redistribution subject to AIP license or copyright, see http://jcp.aip.org/jcp/copyright.jsp

namics (Oxford University, Oxford, 1974).
[26]F. T. Smith, J. Chem. Phys. **31**, 1352 (1959).
[27]R. O. Levine and J. L. Kinsey, in *Atomic–Molecule Collision Theory*, edited by R. B. Bernstein (Plenum, New York, 1979), p. 693 and references therein.
[28]D. A. Case and D. R. Herschbach, Mol. Phys. **30**, 1537 (1975).
[29]A collision complex is assumed for the reaction of $O(^1D) + H_2$: P. A. Whitlock, J. T. Muckerman, and E. R. Fisher, Research Int. Engineering Science Report (Wayne State University, 1976); A. C. Luntz, J. Chem. Phys. **73**, 1143 (1980).

Downloaded 16 Aug 2004 to 129.67.71.67. Redistribution subject to AIP license or copyright, see http://jcp.aip.org/jcp/copyright.jsp